Analysis of the Transient Response of UAV Rotors

S. Al-zubaidi*, and K. Stol
Department of Mechanical and Mechatronics Engineering, University of Auckland, Auckland

http://www.imavs.org/

ABSTRACT

This study presents an analysis of the transient response of Unmanned Aerial Vehicle (UAV) rotors, creating models to predict the transient performance of a rotor through manufacturer-provided data. Understanding the transient response helps in choosing rotors for UAVs in a more accurate manner within optimisation, leading to improved agility and stability of UAVs, in addition to improving simulation tools. The models are validated through different experimental measurements, studying the effect of different rotor properties on the performance of the rotor system. These models can be used to estimate the current within 0.3 A and the rise time within 12 ms, which is restricted by the data logging capabilities. The effect of using different Electronics Speed Control (ESC) protocols on the response was also analysed.

1 INTRODUCTION

There has been a notable rise in utilising Unmanned Aerial Vehicles (UAVs) in different areas over the past few years, such as search and rescue [1] and package delivery. Thanks to technological advancements in electronics, UAVs are now more cost-effective and capable of executing intricate operations, especially for multirotor aircraft. Due to their ability to hover in place, take off, and land vertically, they are highly suitable for performing complex manoeuvres and accessing challenging places.

With the increase in interest, there has been a focus on creating UAV designs that are more optimised for certain purposes. These include different aspects of the design to create efficient [2], more dexterous [3], lighter [4], cheaper [5] and high endurance[5, 6] UAVs. With all these optimisations, the performance of the UAV is assessed around its operating hover conditions. Thus, component models that explain the steady-state performance are sufficient. However, with the increased focus on faster responding UAVs [7, 8] studying the performance of the transient response has become more essential. In addition, unlike conventional UAVs, e.g. quadrotors, which require the UAV to pitch/roll to produce horizontal forces, fully and overactuated UAVs [8, 9] can respond to external disturbance much quicker as their response is dependent on the rotor dynamics only. This makes studying transient response or rotor systems very important.

*Email address: salz167@aucklanduni.ac.nz

The propulsion system performance of UAVs have been studied extensively and verified through experimental methods in [2, 10, 11, 12], with each component of the system studied from its electrical and mechanical properties. While most of these properties are given by the manufacturer, some of the motor and propeller properties required for these models are not readily available, such as the moment of inertia used in [6].

This problem could be solved through two different pathways. The first pathway is to limit the search space within the optimisation. This way, you can buy and test the motors and propellers' performance and use that as the basis for the optimisation [5, 6, 13]. While this is sufficient to prove that the optimisation is working appropriately, it is not practical to be used to identify the best design from a large database of data such as in [8, 9]. In these cases, the problem is solved by assuming motor inertia is negligible compared to the propeller's. While the optimal UAV result might not change, it would provide an inaccurate representation of the performance. In addition, using this method would not be appropriate if the transient response was a constraint for the optimisation as an infeasible UAV could be chosen.

As for Electronic Speed Controllers (ESC), there have been studies [10] that studied their steady-state effect on performance. Still, they have been largely ignored when studying the effect of their properties on the transient phase. A study has tried to investigate the effect of changing controller firmware on performance, finding improvements in response time [14]. Since then, new protocols such as OneShot, Multishot and DShot have been introduced to improve transient performance and accuracy. However, there have yet to be any studies that quantify the improvement seen with these methods.

The main contribution of this paper is the full analysis of the propulsion unit for its transient response, introducing new models for the moment of inertia of the rotor system components. The aim is to enable the estimation of the transient performance of rotor systems using properties manufacturers provide. In addition, the effect of using different communication protocols for the ESC on the transient response will be analysed.

The remainder of this paper is organised as follows. Section 2 introduces the methodology of testing. The different models used are introduced in Section 3. In Section 4, the results of the testing are shown to verify the models. Section 5 outlines the main findings and future work.

http://www.imavs.org/

2 METHODOLOGY

2.1 Test Methods

Different tests have been performed to examine the rotors' performance. The purpose and method of each test are stated below.

2.1.1 Steady-State Test

Within the steady-state test, the rotor is sent a sequence of step inputs and left until the system settles. Data collected is averaged over the last 30 seconds of the response to find the steady-state current, thrust, torque and speed at different levels of ESC inputs.

2.1.2 Step-Response Tests

Within the step-response test, the rotor is sent a sequence of step inputs, figure 1. Data within the transient phase of the response is isolated. This is then used to find the system's response time to different inputs.

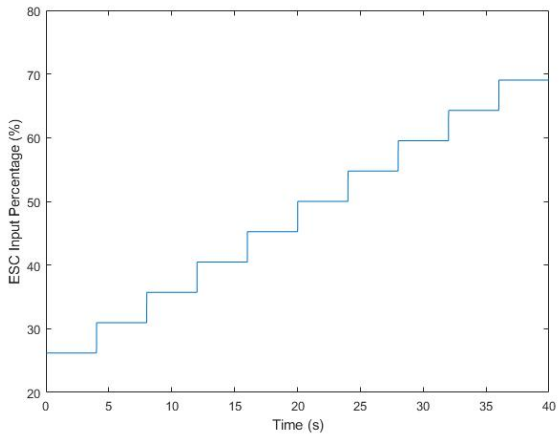

Figure 1: Step-Response Input.

2.2 Data Collection

The response of the propulsion system for different inputs has to be collected. The speed, current, thrust and torque collection were synchronised with the ESC input and collected using the RCbenchmark Dynamometer Series 1580, shown in figure 2. RC Control Board was used to drive the ESC using different protocols. The settings on the Dynamometer were altered to achieve an average sampling rate of 130 Hz. This sampling frequency was high enough to record the transient response. However, the changes in the settings did not improve the torque and thrust sampling rate as a sampling frequency of only 30 Hz was achieved, which is considered insufficient; thus, the thrust and torque must be determined through another method. The RCbenchmark records the torque using load cells placed on the stand. The speed of the motor is recorded using an electrical speed sensor, which involves connecting a probe to one of the wires connecting the ESC to the DC motor.

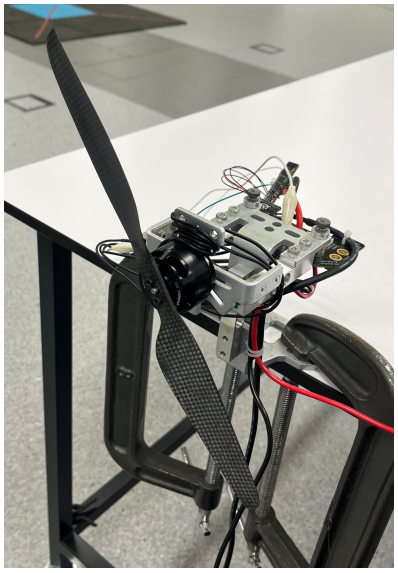

Figure 2: RCbenchmark Test Stand.

3 COMPONENTS

This study defines rotors as the ESC, motor, and propeller systems combined for propulsion within a UAV.

3.1 Propellers

Propellers are responsible for converting the rotational kinetic energy into the thrust required to lift the UAV into the air to hover and perform manoeuvres. The propellers' properties important to consider for this study are torque constant and moment of inertia. Table 1 lists the propellers used in this study.

Propeller	Mass (g)
T-Motor 12" x 4" Carbon Fiber Propeller	14
T-Motor 13" x 4.4" Carbon Fiber Propeller	14.1
T-Motor 14" x 4.8" Carbon Fiber Propeller	15
T-Motor 6" x 2" Carbon Fiber Propeller	1.86
Rctimer TM 6x2 6020 Carbon Fiber Propeller	3
Gemfan F6030 2-Blade Folding Propeller	3.56
HQProp DP 7X4.5 Propeller	6.6
HQProp T5.1X4.5	3.38
HQ T4025	1.45

Table 1: Propellers Used in Case Study.

3.1.1 Torque Constant Model

As the data acquisition rate for torque is lower than that of the other data collected, the torque studied by examining would have to be a theoretical torque. The torque constant relates the rotor load torque with the rotor rotational speed using the common empirical aerodynamic model [9],

http://www.imavs.org/

$$\tau_l = c_{\tau_l}\omega^2 \tag{1}$$

where τ_l is the rotor load torque, ω is the rotational speed of the motor, and c_{τ_l} is the torque constant. The constant is calculated by fitting equation 1 to the speed and torque data collected from the RCbenchmark steady-state experiments. Once the torque constant is found, the torque is assumed to be a function of the speed for the step-response tests. Alternatively, the torque constant could be calculated from the diameter and pitch using equations from [10].

3.2 Motors

The motor converts electrical energy to mechanical rotational energy required for the propeller to generate thrust. In addition to the capabilities of the motor, this study includes a model for the moment of inertia of the motor according to its geometry and mass. Motors are also tested separately to isolate the system before adding propellers. In addition, the testing was performed with motors with quite a large range of speed constants to ensure that the models used are applicable to an extensive range of UAV Motors. Table 2 lists the motors used in this study

Motor	K_V (rpm/V)	D× H (mm)	Mass (g)
Emax ECO II-2004	3000	24.7×19.2	16.4
Emax ECO II-2004	2000	24.7×19.2	16.6
Emax ECO II-2807	1500	33.9×34	46.9
MN1806	2300	23×23.8	18
MN3110	700	37.7×37.1	80

Table 2: Motors Used in Case Study.

3.2.1 Dynamic Response

For the dynamic response, the model used is the one proposed by Magnussen et al. [14, 6]. As per that model, the equation of motion of the rotor is,

$$J_r\dot{\omega} = \frac{K_T}{R}\left(V - K_E\omega\right) - \tau_l \tag{2}$$

where J_r is the rotor moment of inertia, K_T is the motor torque constant, R is the motor internal resistance, K_E is the motor voltage constant, and V is the voltage input. While K_T and K_E are considered equal, the manufacturer does not give them directly but can be derived through the motor speed constant. The equation for this conversion, retrieved from [10], is,

$$K_T = K_E = \frac{V_0 - I_0 R}{K_V V_0} \tag{3}$$

where K_V is the motor speed constant in rad/Vs, V_0 is nominal voltage, and I_0 is the nominal no-load current. Rotor moment of inertia J_r is found through

$$J_r = J_m + J_p \tag{4}$$

where J_m is the motor moment of inertia and J_p is the propeller moment of inertia. The model will be simulated to compare the expected rise time to the experimental data.

3.2.2 Current Model

According to the literature [10], the current through the motor is a function of the voltage, motor parameters and torque. The governing model is

$$I = \frac{V}{V_{in}}\left(\frac{\tau_l K_V V_0}{V_0 - I_0 R} + I_0\right) \tag{5}$$

where I is the current through the motor and V_in is the input voltage.

3.3 ESCs

An ESC is a device that converts the DC voltage from the battery to a three-phase alternating signal required for the brushless DC motors. The effect on the response when using different protocols will be considered. For the rest of the test, *oneshot42* protocol will be used for consistency for the rest of the tests. The ESC used is the Foxeer Reaper F4 128K BL32.

3.3.1 ESC Protocols

The main aim is to understand the effect of different ESC protocols on the response of the rotors. The protocols tested are *PWM50*, *PWM500*, *oneShot125*, *oneShot42*, *multishot*, *dshot 150*, and *dshot300*. *Dshot600* and *dshot1200* was not tested due to the capability of the control module.

4 RESULTS

4.1 Propeller Constant Model

The appropriate motors for each propeller were run at different ESC inputs. Following the procedure from section 2.1.1, steady-state data was extracted. For each propeller, equation 1 were fitted which is evaluated to ensure a proper fit. All of the fits were found to have very low root mean square error (RMSE) and high R^2.

4.2 Moment of Inertia Model

As finding the moment of inertia is quite a complex process, the equations that were suggested within the literature were used to fit the response of the rotor system used. Under this, the assumption was made that the ESC only provides a time delay at the start of the response without having any extra dynamics. This assumption is that the rotor dynamics will only affect the response's rise time. The first-order approximation of the response, from [6], is given by,

$$\frac{\omega}{V} = \frac{K_T}{\tau_r s + 1} \tag{6}$$

where τ_r is the rotor time constant.

$$\tau_r = \frac{J_r R}{K_T^2 + c_{\tau_l} R\omega}. \tag{7}$$

The moment of inertia of each rotor pair is found by performing a fit for each input step and comparing it to its

http://www.imavs.org/

rise time. The relationship between rise time and the time constant is,

$$T_r = 2.2\tau_r \tag{8}$$

where T_r is rise time.

First, the motors were run without a propeller and their moment of inertia was found. Multiple data points for the moment of inertia were found for each motor, and the mean and standard deviation were studied. The data was considered satisfactory as the standard deviation for the moment of inertia was less than 5%. Next, as we aim to find models that depend on data given by the manufacturer, we fit the moment of inertia to the diameter and mass properties. Through that, a fit was found as below,

$$J_m = A_1 + A_2 m_m d_m^2 + A_3 m_m d_m \tag{9}$$

where A_1, A_2, A_3 are constants, m_m is the mass of the motor, and $d_m$is the motor's outer diameter. The constants are found to be $A_1 = 1.77 \times 10^{-5}$, $A_2 = -0.098$ and $A_3 = 2.71$.

Next, the propellers were added to the system, and the same process was followed to find the moment of inertia of the rotor system. The moment of inertia of the propellers was found using equation 4. The data was considered satisfactory as the standard deviation for the moment of inertia was less than 5%.In addition, we also compared the resulting moment of inertia of the same propeller when using different motors to verify the data quality. Within these, the difference between the individual moment of inertia was within 10% which was considered acceptable for the application. Similar to the motor system, a model for the moment of inertia was used, and the fit found is

$$J_p = B_1 m_p d_p^2 - B_2 m_p d_p \tag{10}$$

where m_p is the mass of the propeller, and $d_p$is the propeller's diameter. The constants are found to be $B_1 = 0.135$ and $B_2 = 0.012$.

4.3 Dynamic Response

To verify equation 2, the motor was run through different steps of ESC input. The speed and ESC input are recorded. The ESC input is converted to a reference speed using the equation from [10]. A SIMULINK model is created using the equations 2, and the equivalent voltage was used as input for that model. For each, the experimental data was studied against the results from simulation. Figure 3 shows the response for one rotor, specifically the MN1806 using the T-Motor 6" x 2" Carbon Fiber Propeller. As seen, the two responses match each other quite well.

Next, we ran the motor through multiple steps with equal ESC input increments. The process was repeated 10 times, and the rise time was recorded and compared. Figure 4 shows the comparison, and as we can see, the model works quite well for operating speeds up to 1900 rad/s. The rise time

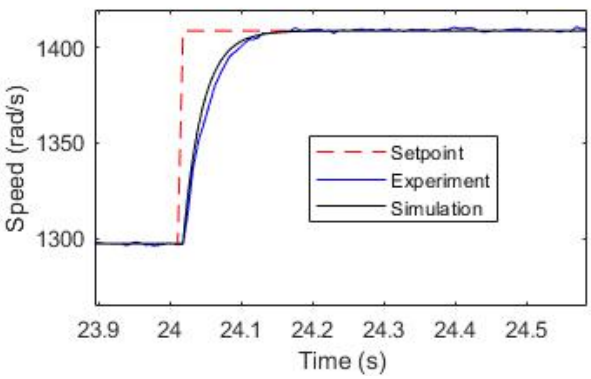

Figure 3: Time Response of One Step

change with operating speed follows a similar trend showing that the models used are quite good. The difference between the experimental and simulated system rise time could be attributed to the limitation in the logging of data. As mentioned above, the average sampling frequency is about 130 Hz, resulting in a sampling period of about 7.7 ms. Looking at the results obtained any over or under-estimation of the rise time was only by about 1-1.5 times that sampling time. While repeating and taking the average reduced the error, small errors are still expected.

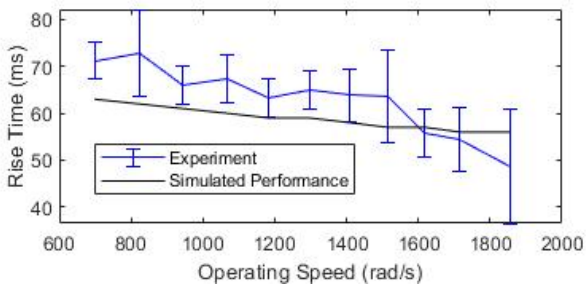

Figure 4: Rise Time at Different Operating Speeds

The same procedure was repeated for the different rotors, and the difference between the expected and actual speed rise times was compared and shown in Table 3 for each trial point. For each rotor, the models used were found to be able to estimate the rise time within less than 1 sampling period with 1 exception. For that rotor system, the rise time was estimated to be within 12.6 ms, translating to only a 6% error.

4.4 Current Response

The appropriate motors for each propeller were run at different ESC inputs. Following the procedure from section 2.1.2, data for each time step has been recorded. The measured current was plotted against the expected current as shown in figure 5 for the Emax ECO II-2807 1500KV motor with the HQProp T5.1X4.5 Propeller. It could be clearly seen

http://www.imavs.org/

Rotor No.	Absolute Difference (ms)	Percentage Difference (%)
1	5.5	9
2	6.1	8
3	4.2	23
4	6.1	16
5	5	12
6	5.3	14
7	7.8	18
8	3	9
9	12.6	6

Table 3: Absolute and Percentage difference between expected and actual rise time

that the current follows the expected current to a very close estimation (within 5%).

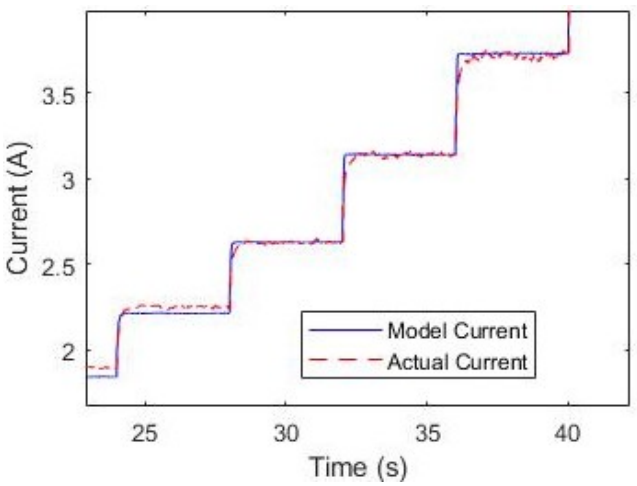

Figure 5: Current Response for Multiple Steps

Secondly, the model was tested with multiple combinations of propeller and motor to verify its performance and validity. For each, the RMSE was calculated between the expected and actual current. As seen in figure 6, 40 trials were conducted of 8 steps, resulting in a maximum RMSE of 0.3 A. This shows that the model provides a good estimation of the current in transient phase.

4.5 ESC Protocols

4.5.1 Dynmaic Response

For the testing of the ESC, we connected the ESC to the MN1806 using the T-Motor 6" x 2" Carbon Fiber Propeller. We tested the system through each of the different input protocols. This was repeated 10 times, and the mean, μ and the standard deviation, σ, of the settling time were recorded. As seen from Table 4, the faster protocols, consistently have the lower settling times, both mean and standard deviation. In

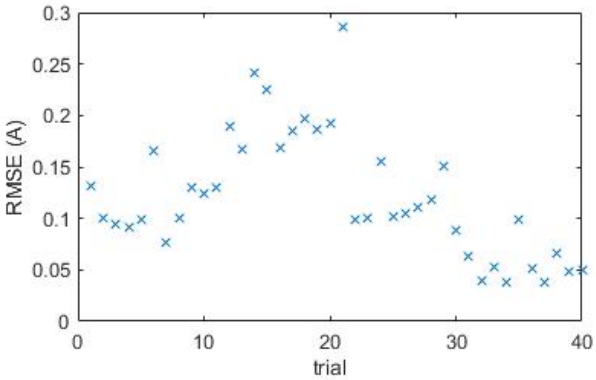

Figure 6: Average current error across trials

Protocol	Step 1		Step 2		Step 3	
	μ	σ	μ	σ	μ	σ
dshot150	101	1.2	98.8	3.5	98.0	3.8
dshot300	105	2.0	103	1.7	99.8	3.1
oneshot42	103	2.9	101	2.2	104	5.3
oneshot125	104	1.6	99.0	8.0	99.4	1.5
multishot	104	1.6	102	4.3	100	6.8
PWM 50Hz	114	4.9	113	7.4	112	7.5
PWM 500Hz	108	2.1	102	4.3	100	9.6

Table 4: Mean and standard deviation of settling time in ms

addition, using PWM at either 50Hz or 500Hz causes an increase in the settling time. This is likely caused by the delay due to the longer signal of 1 ms - 2 ms when using *PWM500* compared to the 125 μs - 250 μs for *oneshot125*. However, the difference in settling time between the different protocols is very small, especially considering systems with propellers of size larger than 4". However, this effect might be magnified when working with much smaller propellers.

5 CONCLUSION

In this paper, the transient performance of the actuation system of multirotor UAVs was analysed. Through only data provided by the manufacturer for off-the-shelf components, the rise time for different steps was estimated within 12.6 ms. This provides a good platform to estimate the performance of these components within simulations and optimisations without requiring the purchase and testing of the components.

For future work, the aim is to use these models of transient response within an optimisation, allowing accurate prediction and extensive search space. In addition, expanding the testing range to other limits to explore different problems

ACKNOWLEDGEMENTS

The research reported in this article was conducted as part of "Enabling unmanned aerial vehicles (UAVs) to use tools in complex dynamic environments UOCX2104", which

is funded by the New Zealand Ministry of Business, Innovation and Employment.

REFERENCES

[1] J. M. Gomez de Gabriel, J. M. Gandarias, F. J. Perez-Maldonado, F. J. Garcia-Nuncz, E. J. Fernandez-Garcia, and A. J. Garcia-Cerezo. Methods for autonomous wristband placement with a search-and-rescue aerial manipulator. In *2018 IEEE/RSJ International Conference on Intelligent Robots and Systems (IROS)*. IEEE, Oct 2018.

[2] X. Dai, Q. Quan, J. Ren, and K. Y. Cai. Efficiency optimization and component selection for propulsion systems of electric multicopters. *IEEE transactions on industrial electronics (1982)*, 66(10):7800–7809, Oct 01, 2019.

[3] D. Brescianini and R. D'Andrea. An omni-directional multirotor vehicle. *Mechatronics (Oxford)*, 55:76–93, Nov 2018.

[4] P. H. M. Souza and K. Stol. Analysis and design of a novel fully-actuated compact multirotor. In *Australasian Conference on Robotics and Automation (ACRA 2021)*, 2021.

[5] O. Magnussen, G. Hovland, and M. Ottestad. Multicopter uav design optimization. In *2014 IEEE/ASME 10th International Conference on Mechatronic and Embedded Systems and Applications (MESA)*, pages 1–6. IEEE, Sep 2014.

[6] Ø. Magnussen, M. Ottestad, and G. Hovland. Multicopter design optimization and validation. *Modeling, Identification and Control*, 36(2):67–79, Jan 01, 2015.

[7] J. Verbeke, D. Hulens, H. Ramon, T. Goedemé, and J. De Schutter. The design and construction of a high endurance hexacopter suited for narrow corridors. In *2014 International Conference on Unmanned Aircraft Systems (ICUAS)*, pages 543–551, 2014. ID: 1.

[8] S. Al-Zubaidi and K. A. Stol. Preliminary design optimisation of a novel fixed-tilt heterogeneous uav for horizontal agility. In *2022 International Conference on Unmanned Aircraft Systems (ICUAS)*, pages 1489–1496. IEEE, Jun 21, 2022.

[9] Z. J. Chen, K. A. Stol, and P. J. Richards. Preliminary design of multirotor uavs with tilted-rotors for improved disturbance rejection capability. *Aerospace science and technology*, 92:635–643, Sep 2019.

[10] D. Shi, X. Dai, X. Zhang, and Q. Quan. A practical performance evaluation method for electric multicopters. *IEEE/ASME transactions on mechatronics*, 22(3):1337–1348, Jun 2017.

[11] X. Dai, Q. Quan, J. Ren, and K.-Y. Cai. An analytical design-optimization method for electric propulsion systems of multicopter uavs with desired hovering endurance. *IEEE/ASME transactions on mechatronics*, 24(1):228–239, Feb 01, 2019.

[12] Z. Czyz, P. Karpinski, and K. Skiba. Experimental study of propellers for the electric propulsion system. In *2021 IEEE 8th International Workshop on Metrology for AeroSpace (MetroAeroSpace)*, pages 682–686. IEEE, Jun 23, 2021.

[13] A. Ayaz and A. Rasheed. Multi-objective design optimization of multicopter using genetic algorithm. In *2021 International Bhurban Conference on Applied Sciences and Technologies (IBCAST)*, pages 177–182. IEEE, Jan 12, 2021.

[14] O. Magnussen, G. Hovland, M. Ottestad, and S. Kirby. Experimental study on the influence of controller firmware on multirotor actuator dynamics. In *2014 IEEE International Symposium on Robotic and Sensors Environments (ROSE) Proceedings*, pages 106–111. IEEE, Oct 2014.

http://www.imavs.org/